Development of Rolling Textures in Aluminum Alloy 3004 Subjected to Varying Hot-Rolling Deformation

P.A. HOLLINSHEAD and T. SHEPPARD

The influence of temperature and strain on texture development in aluminum alloy AA 3004 has been studied in a series of multipass rolling experiments. Temperature had no discernible effect on texture development except through its interactive effects with roll chilling and interpass reheat recrystallization. Some literature-based predictions of rolling textures were in good agreement with the experimental data. The cube texture was formed in small quantities during the interpass reheat recrystallization.

I. INTRODUCTION

IT has been established that dilute aluminum alloys develop a texture of the "copper" or "pure metal" type when rolled.[1] This is primarily due to the high-stacking fault energy of the metal, which ensures that deformation proceeds by slip processes and mechanical twinning does not occur. The development of texture is commercially significant, as it is principally the type and strength of texture which determine the anisotropy of plastic flow in the material during forming operations. An important example of this plastic anisotropy occurs when cups are drawn deep from circular blanks cut from textured sheet. If the plastic flow properties vary with angle around the sheet, the flow of metal will be uneven, and this gives rise to an undulating rim with a number of high points, commonly called ears, and an equal number of low points, called troughs.[2] This manifestation of sheet or planar anisotropy is known as earing. It is well known that rolling textures of the pure metal type impart the tendency for ears to be formed at all positions in the cup, which are oriented approximately 45 deg to the rolling direction (in fact, closer to 48 deg).

The literature has been dominated by results obtained from cold-rolled material, and little attention has been given to the effects of temperature on rolling texture development. A notable exception is the well-documented study by Dillamore and Roberts[1] of the texture transitions between the pure metal and alloy type which occur in copper and α brass with changing temperature.

Aluminum alloy AA 3004 is extensively used in the production of the seamless body in two-piece all-aluminum cans by cupping from sheet, followed by drawing and ironing. A typical fabrication route for the sheet involves direct-chill semicontinuous casting, hot rolling, annealing, and cold rolling to the final gage. In the work reported here, AA 3004 has been rolled to various reductions and various temperatures in the range of 20 °C to 520 °C in multipass schedules. The textures at the midplanes of the rolled pieces were determined, and the results reported.

P.A. HOLLINSHEAD, formerly with the Department of Materials, Imperial College, London, is with the ALCOA Technical Center, Pittsburgh, PA 15069. T. SHEPPARD, Professor of Industrial Metallurgy, is with the Imperial College of Science and Technology, London S.W.7, United Kingdom.

Manuscript submitted June 1, 1988.

II. EXPERIMENTAL METHODS

Aluminum alloy AA 3004, having the chemical composition given in Table I, was direct-chill semicontinuously cast by ALCOA.

The ingot was sectioned into slabs 300 mm long, 65 mm wide, and 48 mm thick. These were homogenized at 600 °C in an air-circulating furnace. Heating and reheating for rolling were also carried out in this furnace, a small thermal head (6 °C at 520 °C, 2 °C to 3 °C at 220 °C) being supplied to compensate for temperature loss during transfer from furnace to rolls. Reductions of 27, 48, 63, 71, 77, and 83 pct were applied at 20 °C, 220 °C, 400 °C, and 520 °C in a multipass rolling schedule. Except for the case of the 20 °C rollings, in which torque and load limitations of the rolling mill necessitated reductions of about 2 mm per pass, the required reductions were achieved in single successive passes. At 20 °C, additional passes were given to total reductions of 90, 96, and 98 pct, and at 220 °C and 400 °C, single additional passes were given to 90 pct reduction. After each pass, except those conducted at room temperature, the slabs were immediately quenched in water in order to avoid recrystallization. Specimens for pole figure determination were extracted from the midthickness of the slabs at 48 pct reduction and at each subsequent reduction. Reheating between passes varied between 30 and 60 minutes, according to the gage. The 300-mm-diameter rolls were heated to 80 °C in an attempt to alleviate the atypical experimental effect of roll quenching. Full (111) and (200) pole figures were obtained for each specimen using a combination of the X-ray reflection and transmission methods. Orientation distribution functions (ODF's) were then calculated by computer from the data used to construct the pole figures. The ODF method used was based on a computer program written by Professor Brent L. Adams of Yale University, New Haven, CT, and extensively modified and supplemented at the ALCOA Technical Center, Pittsburgh, PA, by Dr. W.G. Fricke. The exact position and strength of the ODF maxima were determined using a program written by Dr. S. Panchanadeeswaran.

III. RESULTS AND DISCUSSION

A. *Textures in Fcc Metals*

The rolling textures of fcc metals or alloys of low-stacking fault energy are usually characterized by the

Table I. Composition of Alloy Used, Weight Percent

Mn	Mg	Fe	Si	Cu	Ti	Cr, Ni, Zn	Al
1.10	1.01	0.41	0.18	0.12	0.04	<0.01	bal.

presence of one very strong component with the Miller indices {110}⟨112⟩. The dominance of this texture component in rolled brass led to it becoming known as the "brass" or "alloy" texture[1] and, hence, {110}⟨112⟩ the brass component. On the other hand, fcc metals and alloys of high-stacking fault energy develop a relatively complex rolling texture. A continuous string of orientations is usually formed in such materials, stretching from the brass component through to a component with indices which are close to {112}⟨111⟩. As this type of texture is commonly observed in rolled copper, it has become known as the "copper" or "pure metal" texture[1] and the component commonly termed the "copper" component (Cu). In orientation distribution functions, this continuous string of orientations has been annotated the β fiber.[3] The β fiber does not have a simple, rational description, although it has been described[4] as being close to the fiber obtained by rotation around a ⟨110⟩ axis inclined at 60 deg to the ND in the plane ND-RD (ND = Normal Direction; RD = Rolling Direction).

At low-rolling reductions in high-stacking fault energy materials, texture components may also exist which have {110} planes parallel to the rolling plane (RP) but with various directions parallel to the RD. These types of texture components have been designated as belonging to the α fiber.[3] In Roe's notation,[5] one of the α fibers appears as a straight line on the $\varphi = 0$ deg plane of the ODF at constant $\theta = 45$ deg. This particular α line represents planes of the type $(\bar{1}01)$ lying parallel to the RP, with various directions parallel to the RD; it effectively describes a $[\bar{1}01]$ fiber texture with the ND as the fiber axis.

The rolling textures in aluminum alloys may be characterized adequately by complete descriptions of the α and β fibers.

B. *Rolling Textures in Material Rolled at 20 °C*

The ODF's for the material rolled at 20 °C at each reduction are shown in Figure 1. An example of an α fiber is shown as the dashed heavy line on the $\varphi = 0$ deg section of Figure 1(a), while Figure 2(a) shows the orientation densities along the α fibers for all the 20 °C rolled material. It is clear that at the lowest reduction (48 pct), there are considerable intensities of components along the α fiber with evidence of a peak at about $\psi = 55$ deg, which corresponds to the $(\bar{1}01)[1\bar{2}1]$ brass orientation. With increasing reduction, the brass component increases in intensity and sharpens, and the other components of the α fiber decrease. At 98 pct reduction, the brass component appears to decrease slightly, but this is probably due to either experimental scatter or the intrusion of surface shearing effects into the sheet midthickness at the small final gage of 1 mm.

At the highest reductions, Figure 2(a) indicates that the intensity of the α lines undulates in the region of $\psi = 0$ to 35 deg. These undulations, however, are not genuine representations of the data but are caused by superimposed "ghost" intensities, which often arise as a consequence of the calculation of the ODF by the series expansion method.[6]

Concurrent with the increase in strength at $(\bar{1}01)[1\bar{2}1]$, Figure 2(b) shows the components of texture in the β fiber increase in strength. The intensities of components along each β fiber do not show much variation, although there is perhaps some tendency for these so-called "skeleton lines" to be higher at the extremes of their lengths at the higher reductions. It cannot be said, however, that any true peak tendencies are developing. In dilute aluminum alloys, peaks often may be observed in the skeleton lines about the Cu orientations, {112}⟨111⟩ ($\varphi = 45$ deg in Figure 2(b); *e.g.*, Reference 7) or about the S orientations, {123}⟨634⟩ ($\varphi = 26.6$ deg in Figure 2(b); *e.g.*, Reference 8). Important in determining where the peak develops are (1) the initial texture of the material,[7] (2) the grain shapes, which change throughout deformation and may allow relaxation of certain prescribed shears,[7] and (3) the presence of particles and precipitates.[3] In the work reported here, the initial texture was virtually random, but the alloy did contain a relatively large volume of as-cast constituent particles, approximately 2.5 pct by volume.

Figure 2(c) shows the exact positions of the skeleton lines. It is seen that they do not vary significantly with strain. The skeleton lines, therefore, all tend to pass through similar orientations, namely, {101}⟨121⟩ (brass), {314}⟨485⟩-{427}⟨232⟩ (S), and {326}⟨232⟩-{225}⟨554⟩ (near Cu). Figure 3 suggests that this is a reasonable representation of the orientations present in the material.

At low to moderate reductions, the textures at $\varphi = 45$ deg correspond most closely to the orientation $(\bar{2}25)[554]$. With subsequent reductions in the range of 90 to 98 pct, however, the texture moves toward the Cu orientation $(\bar{1}12)[1\bar{1}1]$.

C. *Material Rolled at 220 °C*

Figure 4(a) shows the α fibers for the material rolled at 220 °C. The brass component $(\bar{1}01)[1\bar{2}1]$ shows a general increase with increasing reduction, although this does not occur as smoothly as observed in the 20 °C material (Figure 2(b)). The intensity levels, however, are often very similar for the two rolling temperatures at equivalent reductions, as is seen by comparing the lines for 48, 77, and 83 pct reductions in Figures 2(a) and 4(a). Figure 4(b) shows the β fiber strengths for the material rolled at 220 °C. These show the same characteristics as observed for the α fibers, *viz.*, a general increase in strength with increasing reduction, occurring not as smoothly as in the 20 °C rolled material (Figure 2(b)) but with similar strengths to the 20 °C rolled material at several reductions, *e.g.*, 48, 77, and 83 pct. Additionally, Figures 1(d) and 5 show the very similar ODF's of the materials reduced 77 pct at 20 °C and 220 °C, respectively. It is concluded, therefore, that an increase in rolling temperature from 20 °C to 220 °C does not have

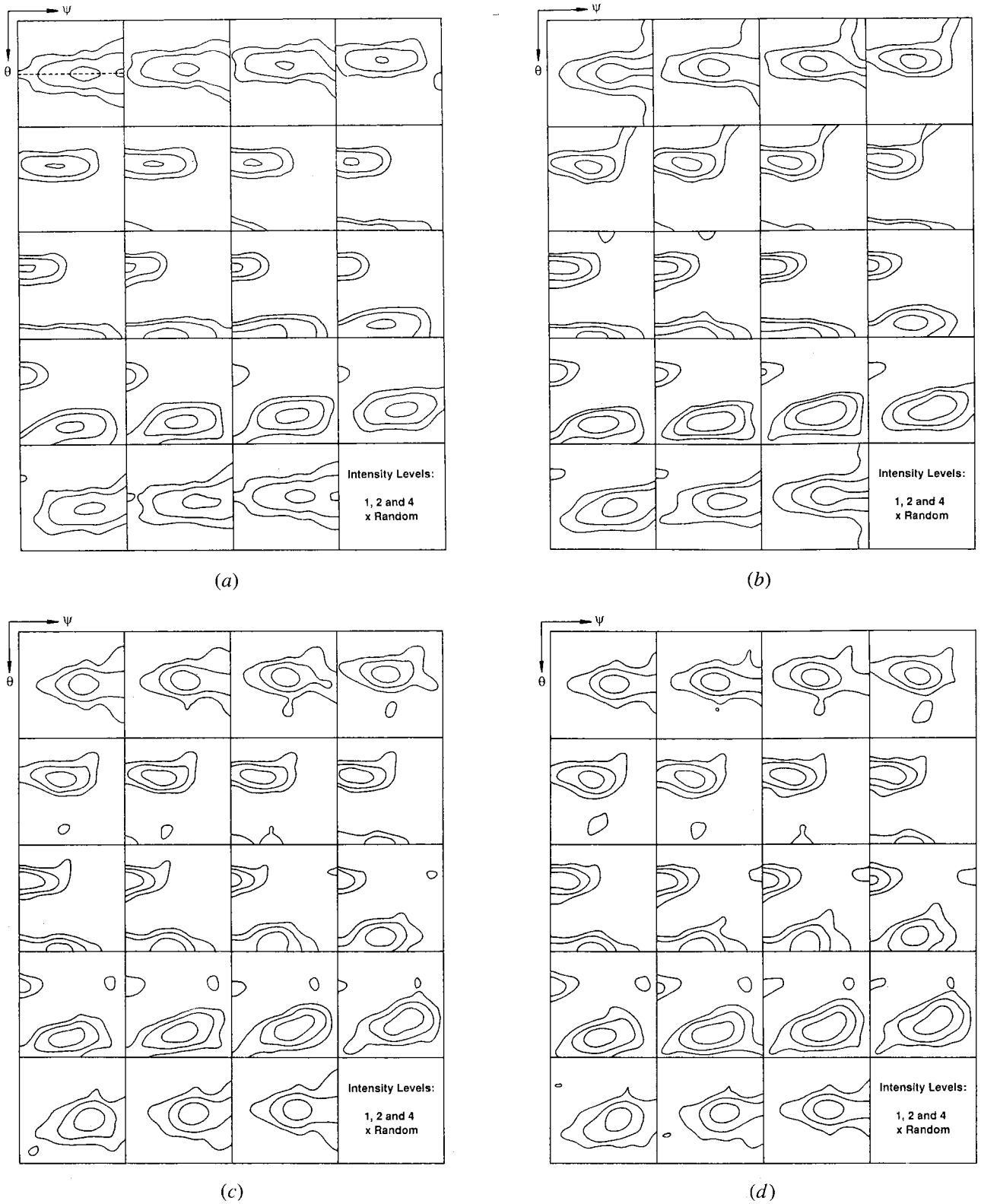

Fig. 1—ODF's in φ = 5 deg increments of material rolled at 20 °C: (*a*) 48 pct reduction; (*b*) 63 pct reduction; (*c*) 71 pct reduction; (*d*) 77 pct reduction; (*e*) 83 pct reduction; (*f*) 90 pct reduction; (*g*) 96 pct reduction; and (*h*) 98 pct reduction.

any significant effect on the type or strength of the texture components produced. The smoother buildup of texture in the 20 °C rolled material may be attributed to the "averaging" effect of the greater number of passes, which was required to achieve a given reduction for this case. Inconsistencies in the texture buildup in any one rolling pass due to disturbances to the symmetry of the rolling stresses, perhaps due to surface friction variations between the top and bottom rolls, could be corrected in the subsequent passes before the desired gage was reached.

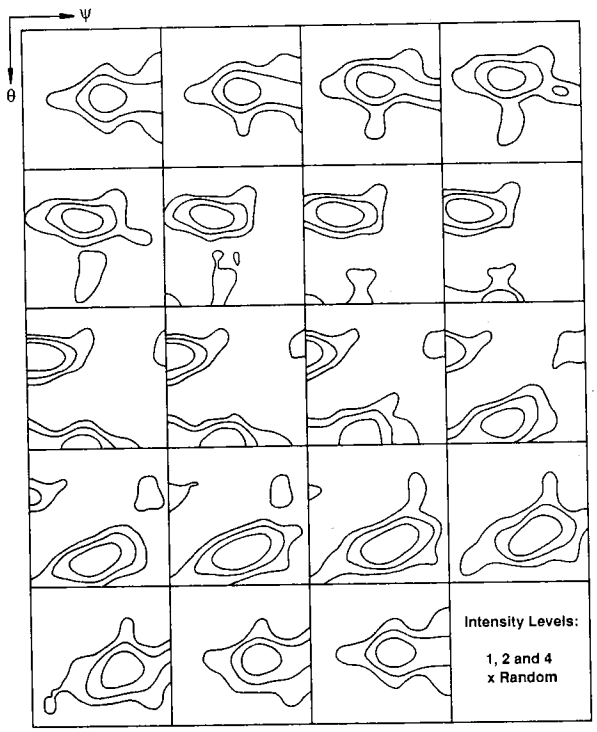

(*e*)

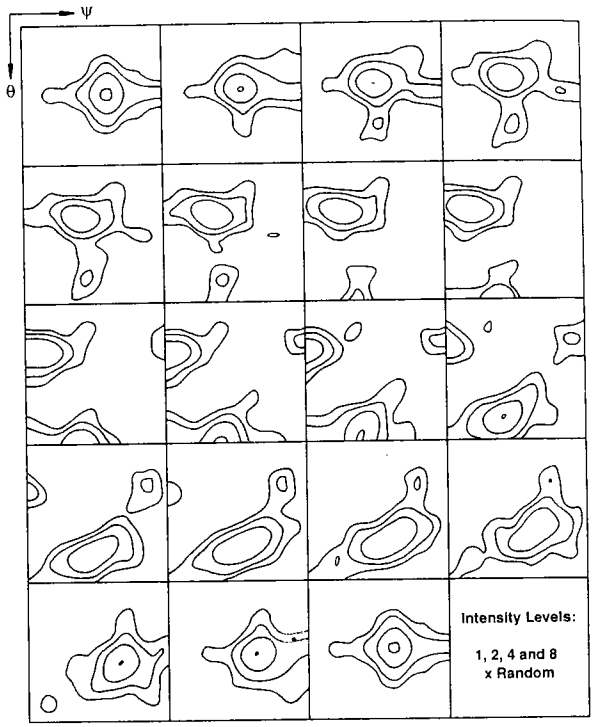

(*f*)

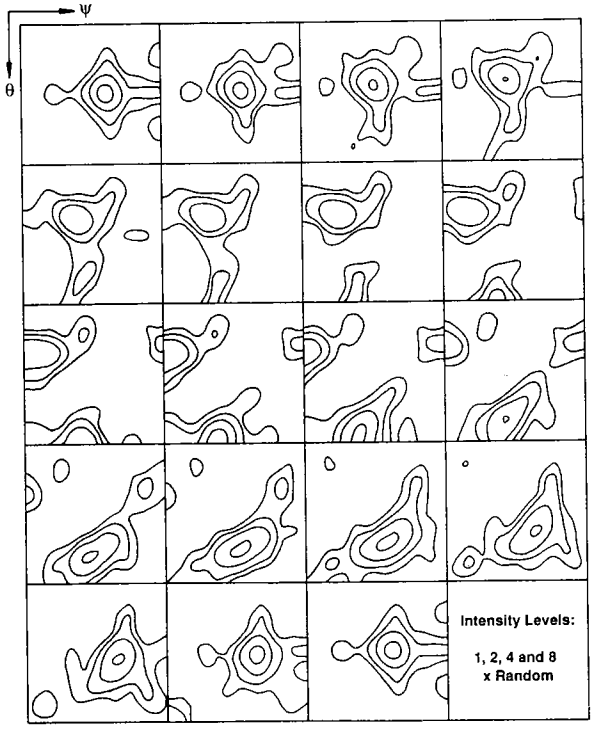

(*g*)

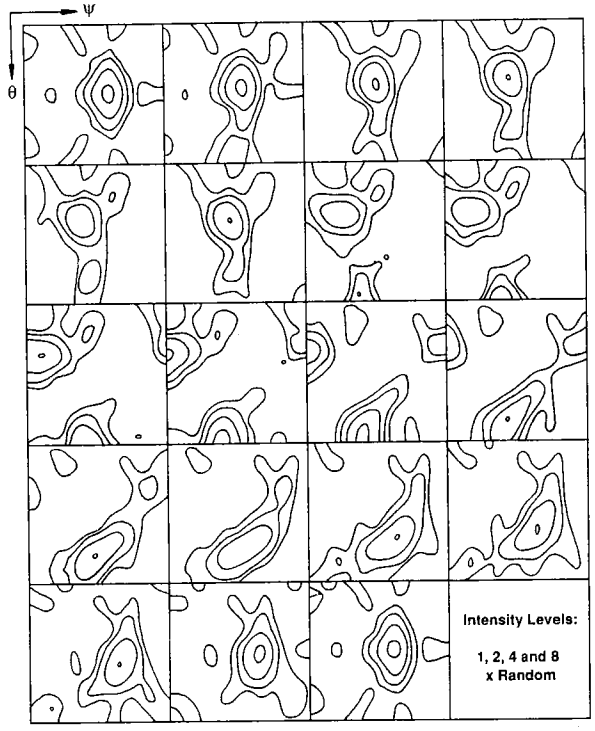

(*h*)

Fig. 1 Cont.—ODF's in φ = 5 deg increments of material rolled at 20 °C: (*a*) 48 pct reduction; (*b*) 63 pct reduction; (*c*) 71 pct reduction; (*d*) 77 pct reduction; (*e*) 83 pct reduction; (*f*) 90 pct reduction; (*g*) 96 pct reduction; and (*h*) 98 pct reduction.

In the 220 °C rolled material, on the other hand, the desired gages were reached in single successive passes, and any such texture inconsistencies produced would still exist at the sampling stage. Indeed, it has been shown very recently[9] that when curvature is produced during the rolling of aluminum, the normal pure metal-type texture becomes distorted. Despite the fact that all materials with anything other than slight curvature were rejected in this work, small distortions of the texture data still occurred. This was especially true at the low reductions.

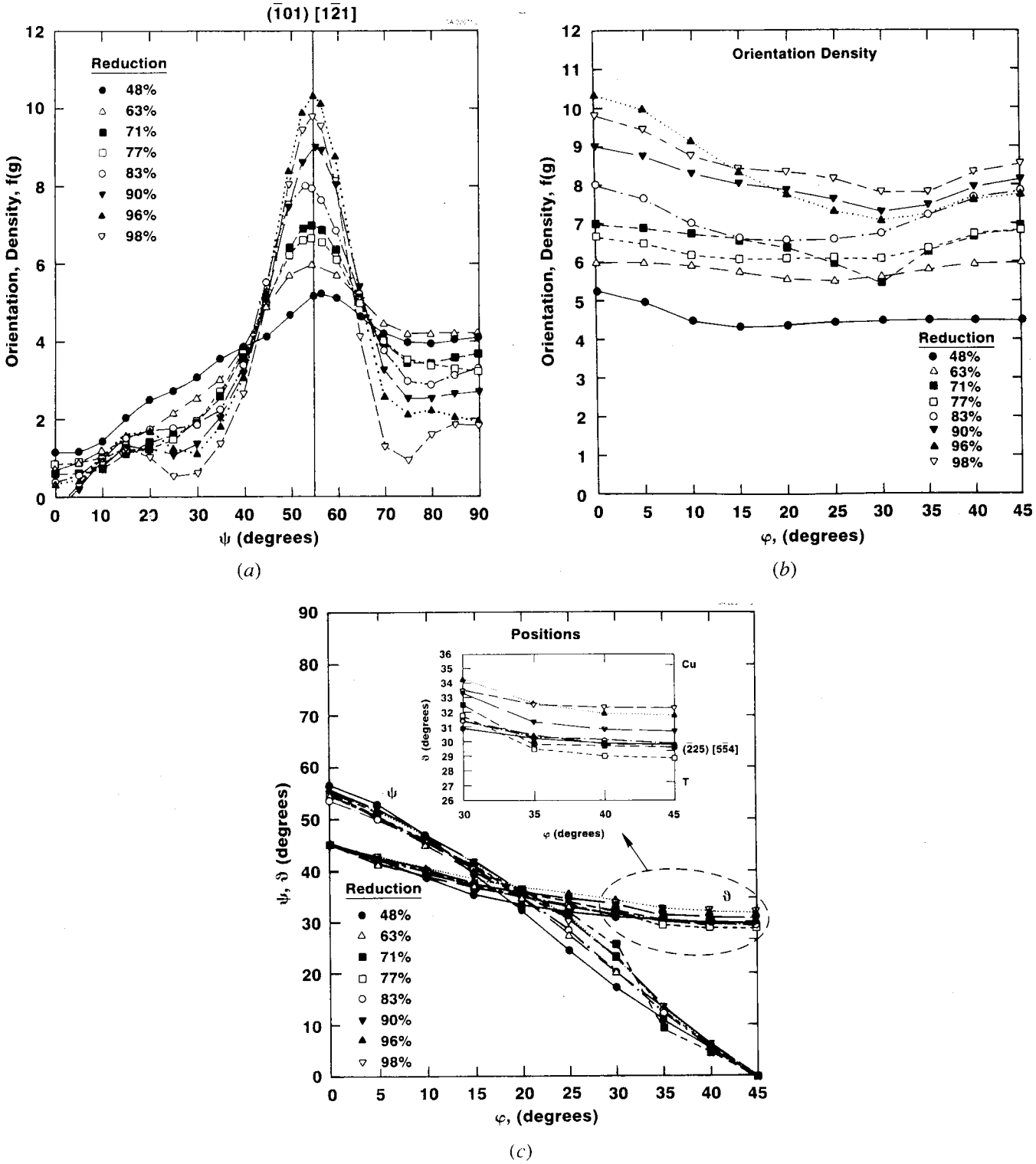

Fig. 2—ODF data for material rolled at 20 °C: (*a*) strengths of α fibers; (*b*) strengths of β fibers; and (*c*) positions of β fibers.

For example, examination of Figure 4(b) clearly shows that there are discontinuities in the β fibers at the two lowest reductions.

There is no evidence that the θ values increase with reduction (as at 20 °C; at $\varphi = 45$ deg, the component is almost exactly $(\bar{2}25)[554]$ in every case). The reader should note, however, that the maximum reduction was 90 pct for this material, and Figure 2(c) shows that for 20 °C rolling, the shifts become observable only at higher reductions.

D. *Material Rolled at 400 °C*

Figure 6(a) shows the α-fiber strengths of the material rolled at 400 °C, while Figures 6(b) and (c) show the β-fiber strengths and the β-fiber positions, respectively,

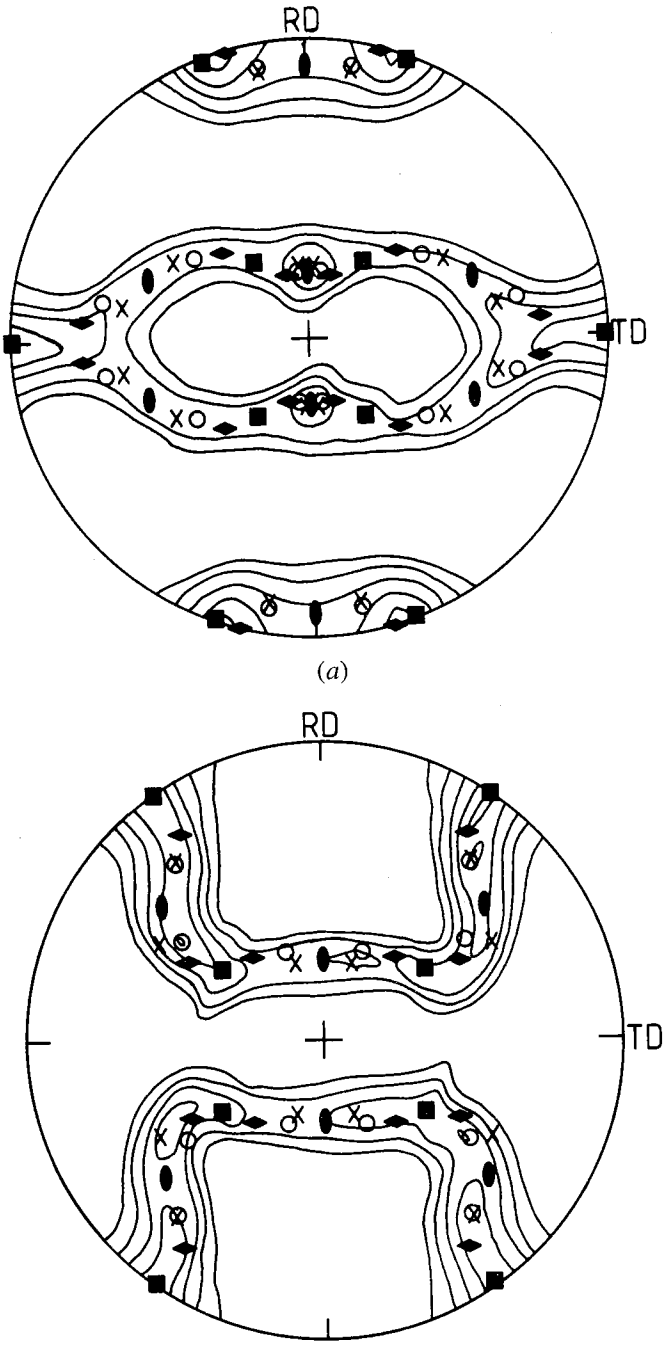

Fig. 3—Pole figures of material rolled 98 pct at 20 °C: (*a*) (111) pole figure and (*b*) (200) pole figure.

for the same material. Compared to the data for lower temperatures, the evolution of texture appears to be more complex. For example, at 48 pct reduction, the α fiber shows two peaks and, correspondingly, the β fiber is split in the range $\varphi = 0$ to 10 deg. This result is most probably caused by varying oxide film thicknesses on the top and bottom faces of the material, thus creating differing friction conditions at each roll. The result is an asymmetrical stress distribution about the central plane, thus causing a distortion of texture.

At higher reductions, the α and β fibers appear to be consistent with lower temperatures, but the texture strength increases only up to 77 pct reduction, followed by a decay. This is due to the occurrence of interpass reheat recrystallization and its complex interaction with the effects of roll chilling. Figure 7(a) shows that during the reheat following the first pass (27 pct reduction), some very small recrystallized grains appear at the grain boundaries and at some of the constituent particles. At these low reductions, the amount of interpass reheat recrystallization is small but must have the tendency to decrease the rate of texture development. When rolling at higher temperatures, the relatively cold work rolls chill the outer layers of the slab, stiffening them, accentuating deformation in the unchilled softer central layers and, hence, increasing the midthickness texture strength. At low reductions, therefore, the texture strength may show a general increase in strength with increasing reduction: at 77 pct reduction, the texture strength of the 400 °C rolling is greater than for both of the lower temperature rollings. When greater deformation is effected, however, roll chilling clearly will not have the same effect. Under such conditions, the chilling effect of the rolls may penetrate as far as the midplane in the latter part of the roll bite, and deformation then takes place at a lower temperature than indicated. This midplane material is, consequently, very prone to recrystallize during the reheat for the next pass. Thus, in the material rolled at 400 °C, the maximum texture strength was observed at 77 pct reduction, but extensive recrystallization took place during the subsequent reheat (Figure 7(b)). The texture developed during the subsequent pass to 83 pct reduction could not compensate for this, and so the texture was weaker than at 77 pct reduction. Following the pass to 83 pct reduction and reheating, the material appears to be over 50 pct recrystallized (Figure 7(c)). Because of this interpass reheat recrystallization, any comparisons of the ODF's for these higher temperature schedules with those deformed at 20 °C and 220 °C would not be instructive. This sequence of events is supported by the data presented in Figure 8, which shows the texture severity parameter plotted against strain. The texture severity parameter, J, indicated the texture strength was developed by Kallend[10] and, in effect, may be regarded as the standard deviation of the ODF from that of a random material, where

$$J = 4.2^{0.5}\pi^2\left[\sum_{l=1}^{\infty}\sum_{m=-l}^{l}\sum_{n=-l}^{l} W_{lmn}^2\right]^{0.5}$$

At the lowest reductions, the texture strength in the 400 °C rolling develops in much the same way as for the lower temperature rolling. In the reheats for the last two phases, however, the interpass reheat recrystallization exerts a greater influence than the roll chilling effect, and the texture severity parameter decreases accordingly.

E. *Material Rolled at 520 °C*

Figure 9 indicates that rolling at 520 °C produces similar features to those observed at 400 °C, except that the effects of roll chilling and interpass recrystallization are

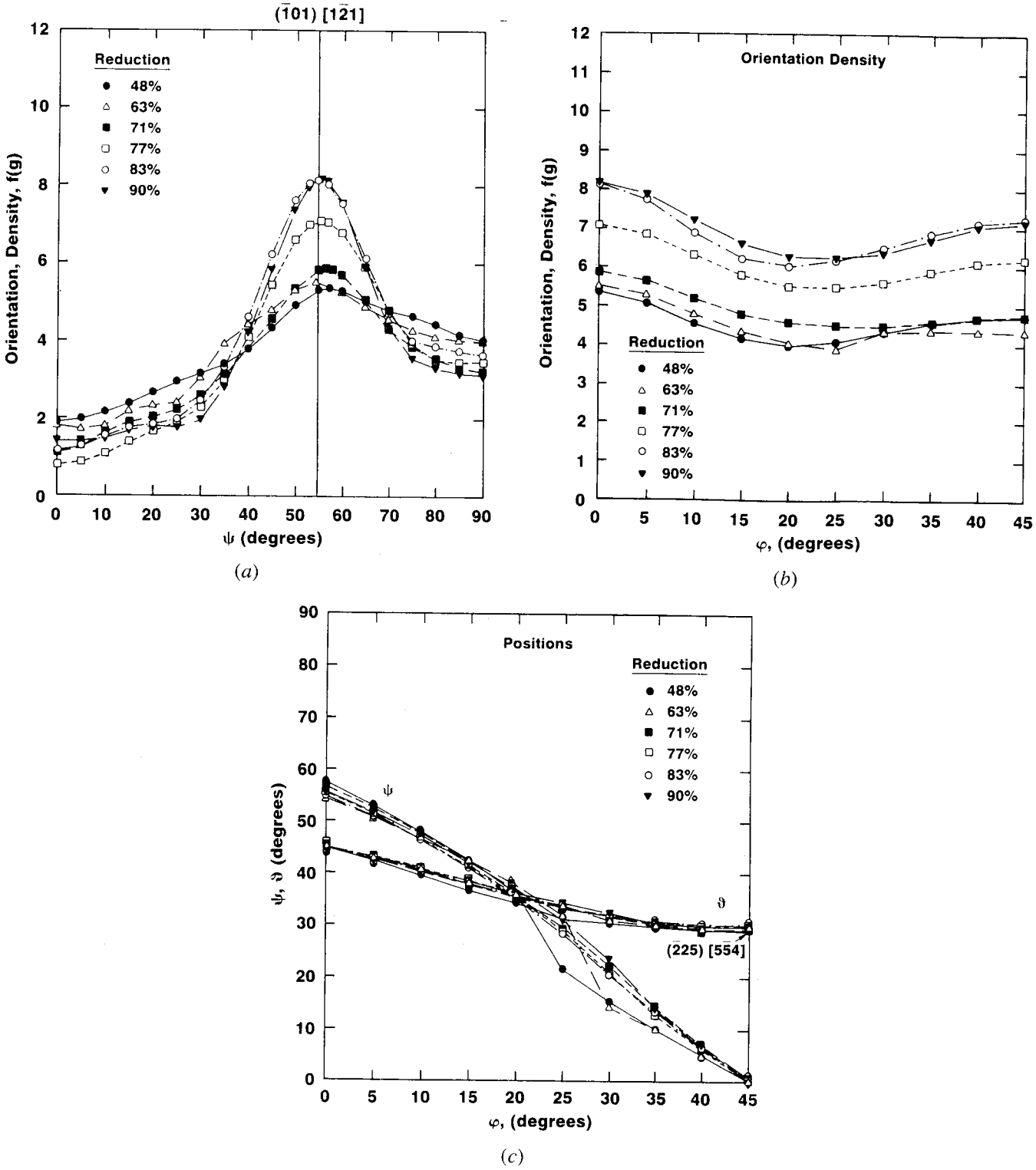

Fig. 4—ODF data for material rolled at 220 °C: (*a*) strengths of α fibers; (*b*) strengths of β fibers; and (*c*) positions of β fibers.

accentuated. Indeed, at the lowest nominal reductions, the highest texture severity parameters were obtained at 520 °C, due to the very steep temperature gradients developed in the slabs and the resultant concentration of the deformation at the midplane. The roll chilling at 520 °C, however, permeates the midplane at a higher gage than at 400 °C; thus, the texture strength drops at a lower strain. The appearance of the α fiber and the strengths and positions of the β fiber are shown to be complex in Figures 9(a), (b), and (c), respectively. Figure 9(a) shows that the peaks in the α fibers appear to be random. As discussed above, this is assumed to be due to the problems associated with the thick oxide film developed on the surface of the slabs, the extremely low

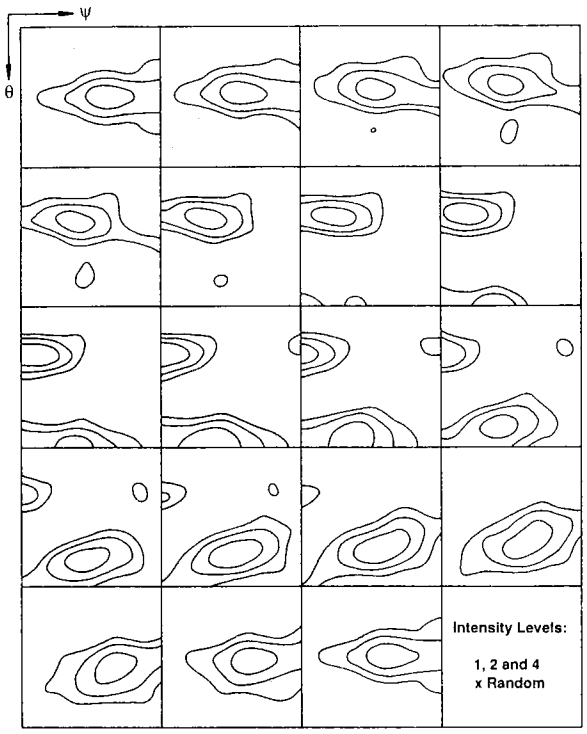

Fig. 5—ODF in φ = 5 deg increments of material reduced 77 pct at 220 °C.

mechanical strength of the slabs at these high temperatures, and the interpass reheat recrystallization.

Figures 9(b) and (c) show that the β-fiber strengths and positions are also unsystematic. Very noticeable, however, in comparing Figure 9(b) with Figures 2(b), 4(b), and 6(b), is the apparent reinforcement of the orientations about $\varphi = 0$ deg in the material rolled at 520 °C. Some explanation is required to account for this. A possibility is that at such a high deformation temperature, the fundamental model of deformation may change. This could be hypothesized on the basis of recovery occurring, with climb being more prevalent than at lower temperatures. A much more plausible explanation, however, is that the brass orientation is formed as a direct or, more likely, indirect result of the interpass reheat recrystallization; it has been reported[12] that in cold-rolled single crystals of copper, different orientations were more or less susceptible to recrystallization. It was noted that the brass orientation was particularly resistant to recrystallization. In the present case, therefore, it is postulated that the brass components of the rolling texture recrystallize to only a small degree relative to other orientations of the rolling texture during the interpass reheats. At least some of the recrystallization occurring in other orientations could result in orientations which are either close to the brass components or are orientations which rotate readily toward these on subsequent deformation, thus causing a reinforcement of the brass component after deformation.

Additional evidence of the occurrence of interpass reheat recrystallization in the material rolled at 400 °C and 500 °C is found in the cube texture strengths of the ODF's of each of the specimens studied (Table II). It is seen that the cube texture strengths of the material rolled at 20 °C and 220 °C, in which no interpass recrystallization was observed to occur, are, in general, below random intensity, *i.e.*, $<1 \times R$. The values for these materials oscillate with strain, and this reflects the uncertainty in the absolute values at such low densities. Nevertheless, it is clear that the cube texture strengths for some of the 400 °C and 520 °C rollings are significantly above random levels. Clearly, therefore, the cube textures were being formed in some measurable quantities by recrystallization during the interpass reheats. The ODF for the material reduced 83 pct at 520 °C is shown in Figure 10, and this clearly shows the presence of the cube texture, most easily seen at the corners of the $\varphi = 0$ deg section.

F. *Rate of Rolling Texture Evolution*

Figure 8 also gives some indication of the rate of texture evolution during cold rolling. For the material rolled at 20 °C, it is seen that the rate of increase in the texture severity parameter decreases with increasing natural strain. This suggests that the initial rotations of any general orientations toward the string of pure metal-type rolling texture components are initially quite rapid, but as the orientations approach these "stable" endpoints, the rates of rotation become progressively slower. Thus, at the highest strains, the slope of the line for the 20 °C rollings tends toward zero.

G. *Comparisons of Experimental Textures with Model Predictions*

Hirsch and Lücke[4] have modeled the evolution of texture under the conditions of imposed stress (Sachs model[13]) and imposed strain (Taylor model[14]). The Sachs model simulations were formulated using Kochendorfer's assumption[15] that all the grains deform by the same amount in the compression direction; however, it is called the "no constraints" model (N model), since only the principal thickness reduction was imposed by using the external (Tucker[16]) stress state. The Taylor model was used either fully constrained (F model), *i.e.*, with five independent shears required to fulfill the imposed plane strain conditions, or with relaxation of various shear components of the imposed strain tensor. Some of Hirsch and Lücke's predictions of the β-fiber positions at $\varepsilon = 1$ and 3 are reproduced in Figures 11(a) and (b), respectively.

At low reductions, all models predict a buildup of intensities along both the α and β fibers. The N model also predicts a peak corresponding to the brass component at $\varepsilon = 1$. Comparing the β-fiber positions of Figures 2(c), 4(c), 6(c), and 9(c) with Figure 11(a), however, shows that the F model gives a better prediction of the orientations formed than does the N model. It would appear, therefore, that the material initially deforms under mainly Taylor-type conditions. Some Sachs-type deformation conditions could also be taking place, perhaps at the grain interiors, and this could explain the experimentally observed peaks at the brass orientation.

As deformation proceeds, the grains become progressively flattened and elongated. Grain interiors could then no longer act independently of the rest of the grain, and

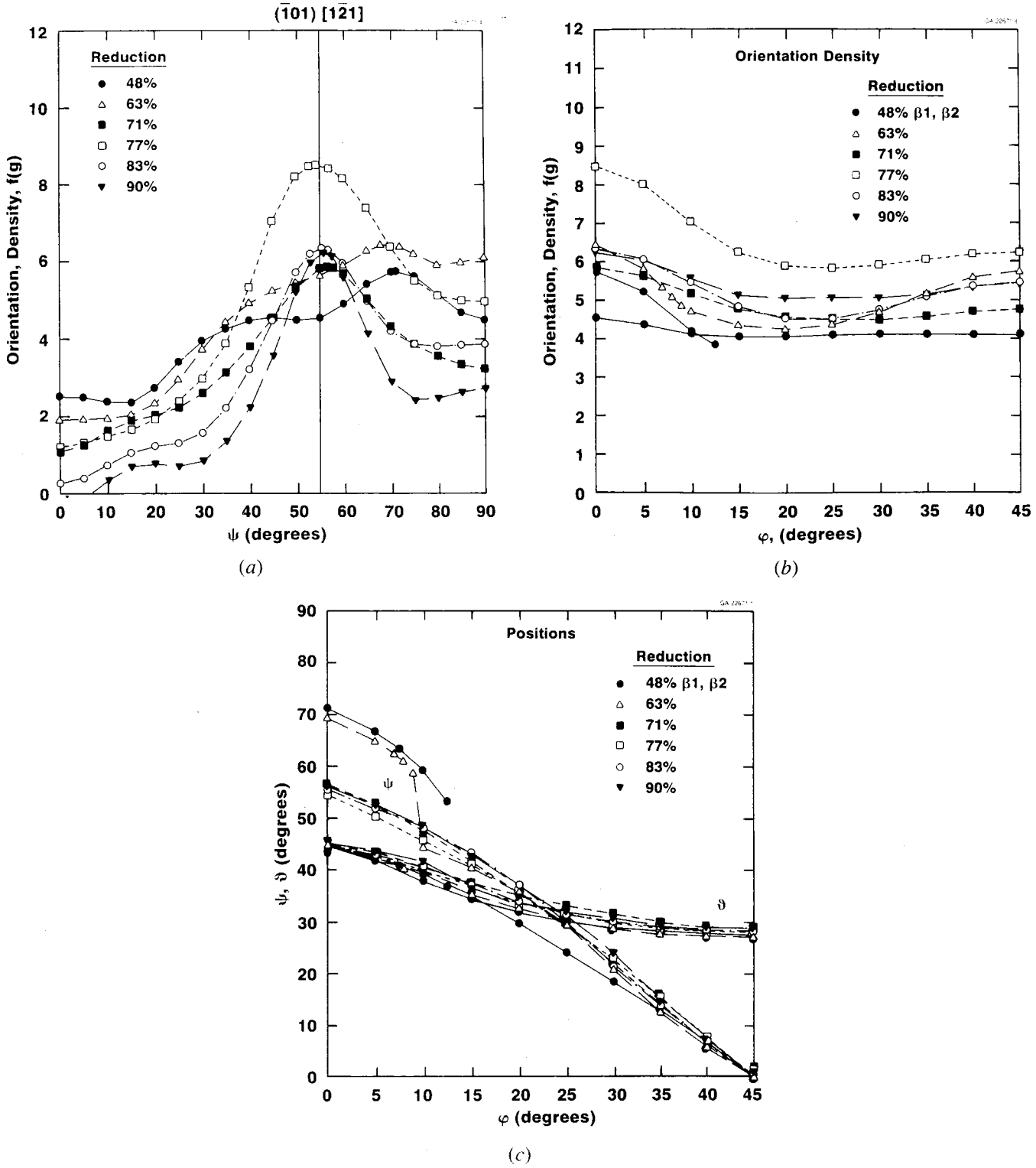

Fig. 6—ODF data for material rolled at 400 °C: (*a*) strengths of α fibers; (*b*) strengths of β fibers; and (*c*) positions of β fibers.

so any Sachs-type deformation conditions would be expected to give way to the more constrained Taylor-type conditions. Furthermore, the grain shapes are then such that ε_{NR} and ε_{NT} shears are feasible (for example, ε_{NR} = shear on plane perpendicular to the normal direction in the rolling direction; T = transverse direction). The consequence is a relaxation of some of the constraints of the F model. Hirsch and Lücke showed that relaxation of the ε_{NR} in the F model produced results very similar to the F model. The peak intensity, however, was closer to the true copper (Cu) orientation, $\{112\}\langle 111\rangle$ (at ψ = 0 deg, θ = 35 deg, and φ = 45 deg), instead of the T orientation (at ψ = 0 deg, θ = 27 deg, and φ = 45 deg), and the model, thus, was called the C model. Similarly,

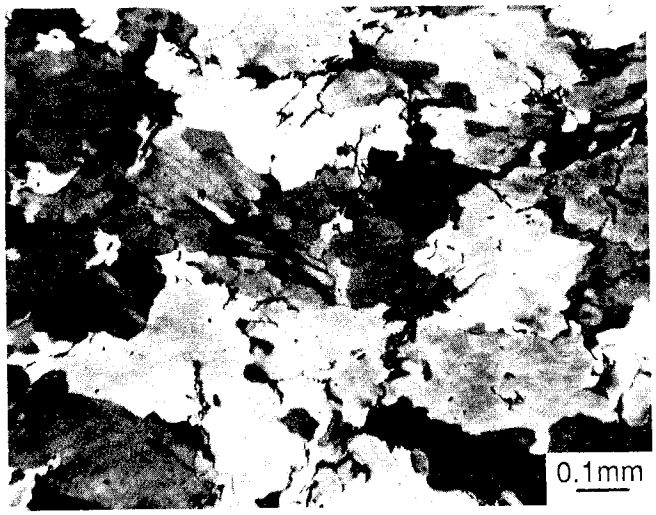

(*a*)

(*b*)

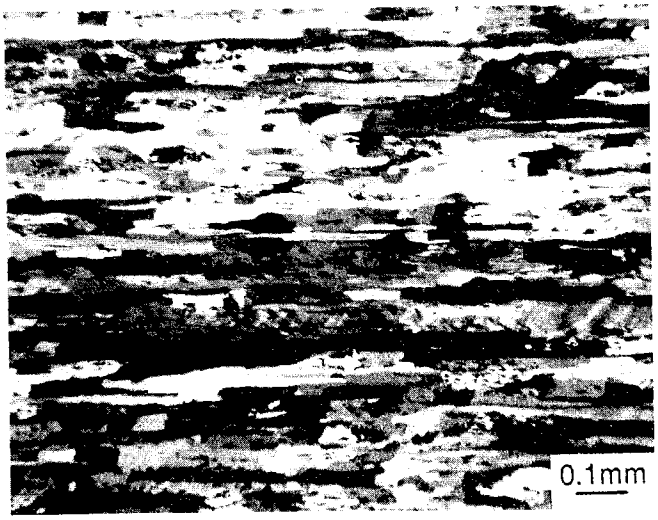

(*c*)

Fig. 7—Optical micrographs of material rolled at 400 °C. Longitudinal sections anodized and examined under polarized light: (*a*) reduced 27 pct and reheated for next pass; (*b*) reduced 77 pct and reheated for next pass; and (*c*) reduced 83 pct and reheated for next pass.

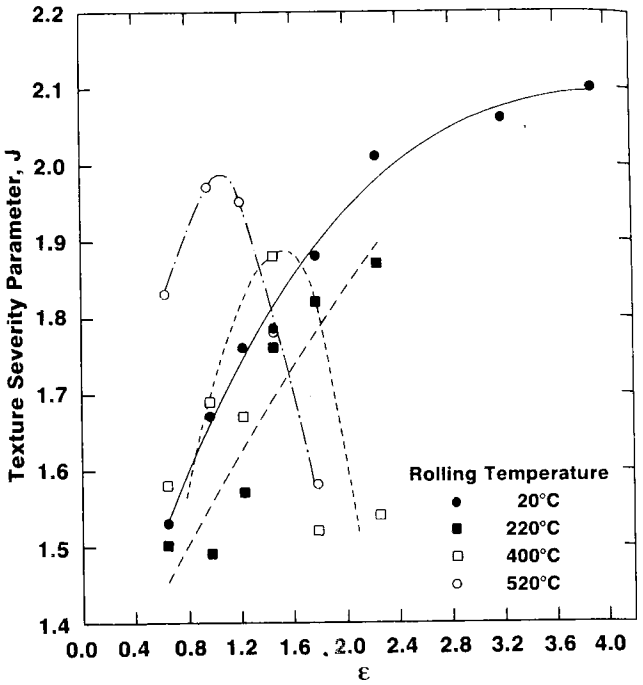

Fig. 8—Graph of texture severity parameter J against strain for all rolling temperatures and reductions.

ε_{NT} shears gave the T orientation, with spread toward the S component, $\{124\}\langle 12\ 8\ 7\rangle$ (at $\psi = 28$ deg, $\theta = 29.2$ deg, and $\varphi = 28$ deg), thus being annotated the S model. A combination of ε_{NR} and ε_{NT} shears (SC model) gave both the Cu and S components. Hirsch and Lücke's predicted β-fiber position for $\varepsilon = 3$ is shown in Figure 11(b).

Comparison of the 20 °C rolling data of Figure 2(c) with Figure 11(b) shows that the F model still gives a good prediction of the positions of the experimental skeleton lines, and it predicts an orientation close to the brass component at $\varphi = 0$ deg. It must be emphasized, however, that the brass component predicted by the model is very weak and the texture is heavily biased toward the T component $\{4\ 4\ 11\}\langle 11\ 11\ 8\rangle$. Indeed, none of the models represented in Figure 11(b) predicts any appreciable brass component strengths. If, however, ε_{TR} shears are allowed to occur, an appreciable brass component is predicted. A problem exists in that ε_{TR} shears really only are feasible at low reductions or in special orientations which are able to find a way to accommodate these shears.[4] The inability to predict an appreciable brass component in the absence of ε_{TR} shears has been a shortcoming of such Taylor-based models. "Self-consistent" approaches such as that by Molinari *et al.*,[17] in which the effects of nearest-neighbor grain interactions are taken into account, show some improvement in this respect, but no ODF data appear to be available yet for direct comparison with experimental results.

The S model (ε_{NT} shears allowed) gave similar predictions to the F model except at $\varphi = 0$ deg. The C model (ε_{NR} shears allowed) also gave reasonable predictions, except that the ψ line was shifted to somewhat higher values in the range $\varphi = 0$ deg to about 20 deg. The SC model (ε_{NT} and ε_{NR} shears allowed) appears to give

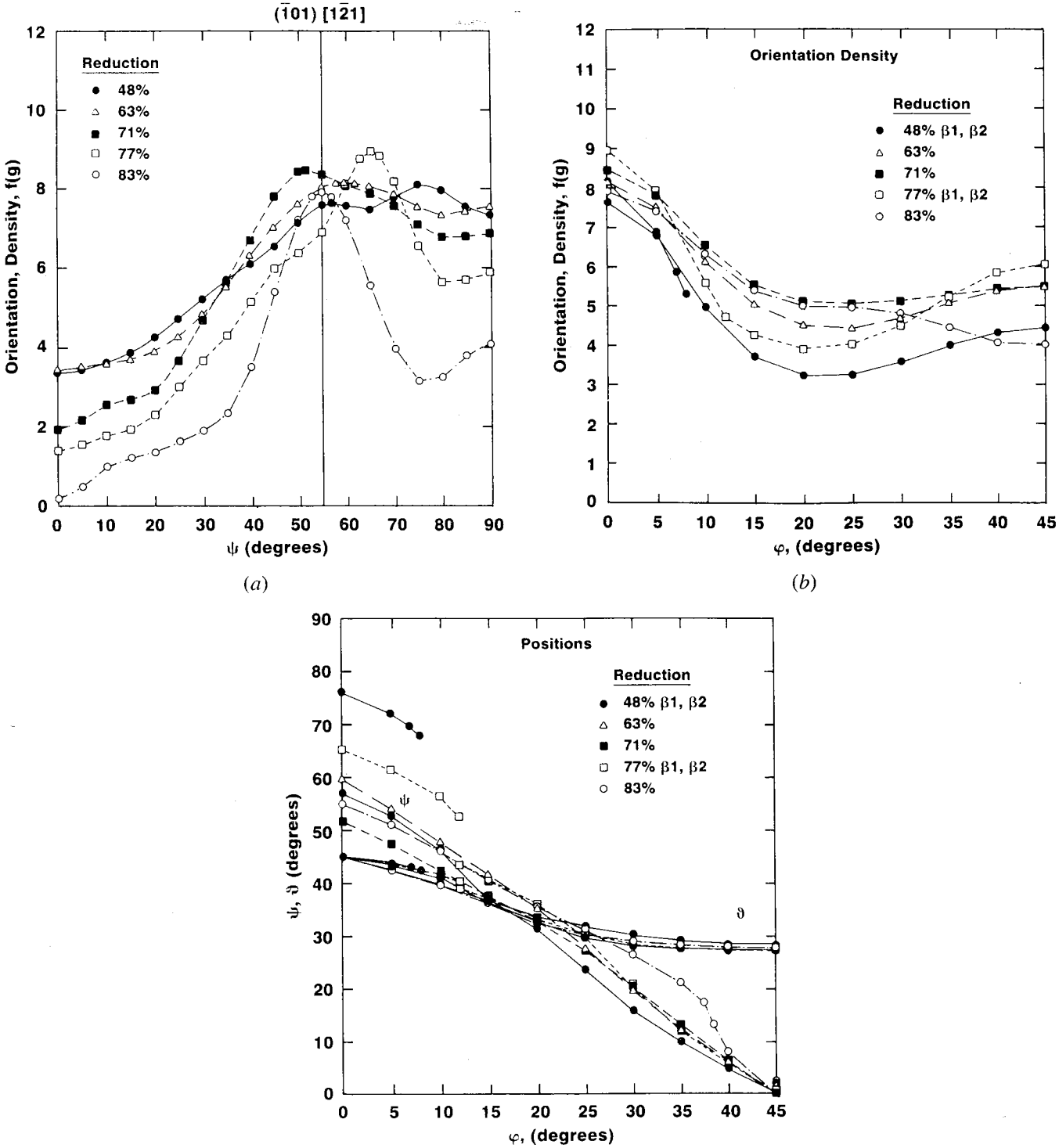

Fig. 9—ODF data for material rolled at 520 °C: (*a*) strengths of α fibers; (*b*) strengths of β fibers; and (*c*) positions of β fibers.

Table II. Cube Texture Strengths in As-Rolled Material

Rolling Temperature	Reduction							
	48 Pct	63 Pct	71 Pct	77 Pct	83 Pct	90 Pct	96 Pct	98 Pct
20 °C	1.0	1.1	0.5	0.6	0.4	0.3	0.6	0.8
220 °C	0.8	0.9	0.4	0.4	0.5	0.7	—	—
400 °C	0.9	1.2	0.4	1.4	1.4	1.7	—	—
520 °C	1.8	1.6	2.6	1.6	2.9	—	—	—

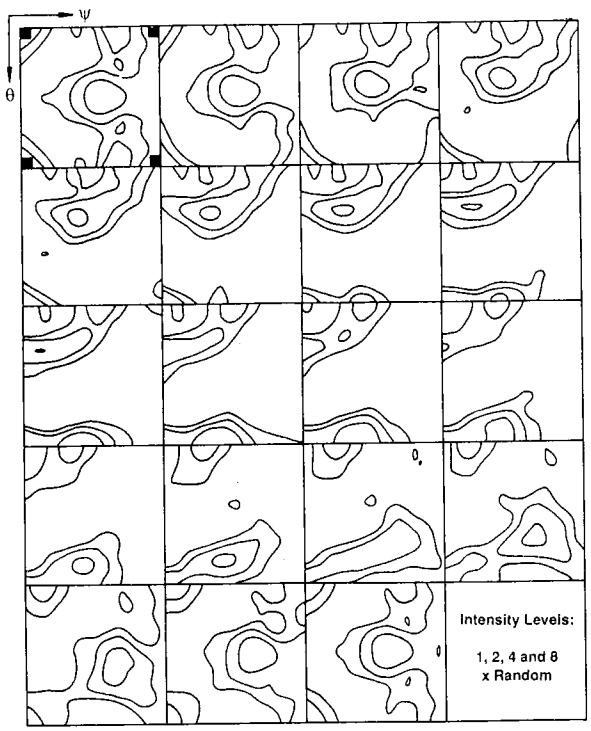

Fig. 10—ODF in φ = 5 deg increments for material reduced 83 pct at 520 °C. Cube texture is shown as ■ on φ = 0 deg section.

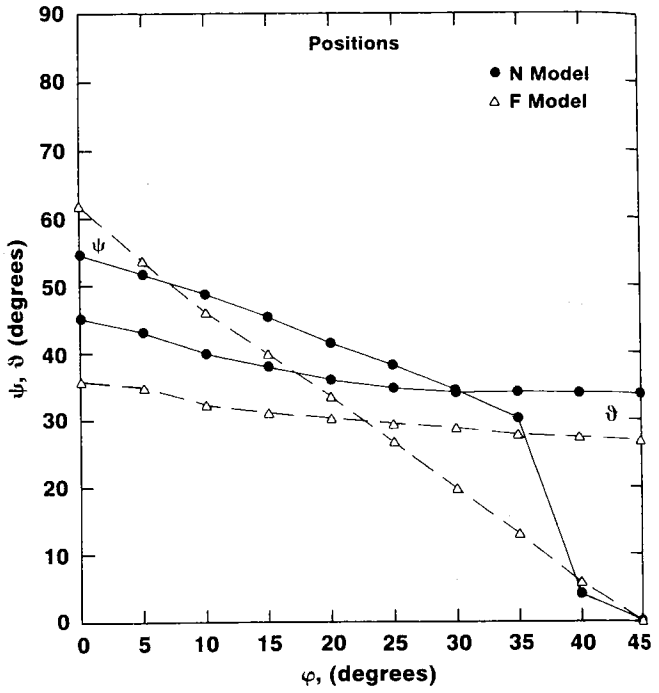

(*a*)

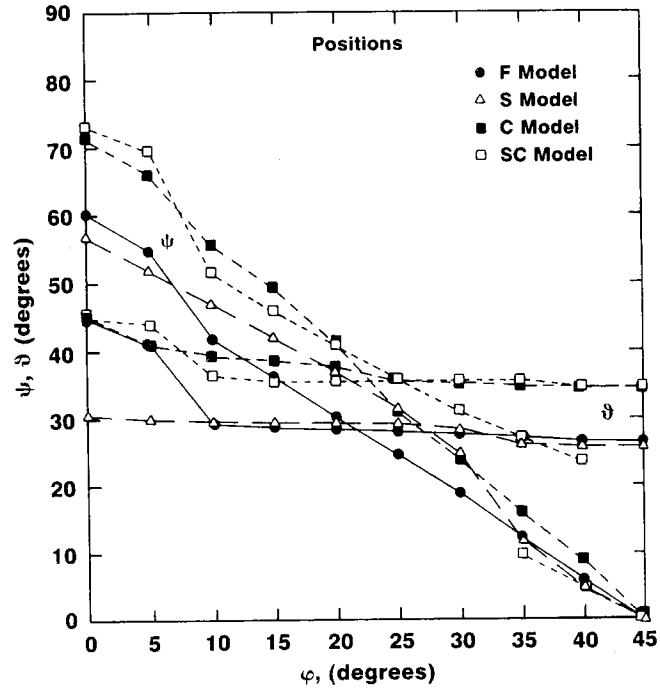

(*b*)

Fig. 11—Model predictions of β fiber positions at (*a*) ε = 1 and (*b*) ε = 3. N model = Sachs imposed stress model; F model = Taylor full constraints model; C model = F model with relaxation of ε_{NR} shears; S model = F model with relaxation of ε_{NT} shears; SC model = F model with relaxation of ε_{NR} and ε_{NT} shears.

the poorest predictions of the models represented in Figure 11(b), but, in reality, the predictions are very similar to those of the C model. The differences in the lines for the C and SC models arise because the latter predicts peaks to occur at both the S and Cu orientations; if a smooth transition between these two orientations were allowed to occur for the SC model in Figure 11(b), the results would appear very similar for the S and SC models.

The trend shown in Figure 2(c) for the positions to increase with increasing reduction may be explained in terms of relaxation of the ε_{NR} shears. As stated above, under F-type conditions, the T component (ψ = 0, θ = 27.2, and φ = 45 deg) is by far the strongest component predicted to occur. The ε_{NR} shears (C model) have the greatest likelihood of occurring, as these have the least problem of grain boundary accommodation in rolling deformation, and so when they are allowed to occur, the Cu component (ψ = 0, θ = 35.3 , and φ = 45 deg) becomes favored over the T component, and the value, therefore, shifts toward 35.3 deg. Although this shift appears to be taking place in the experimental data, it should be noted that the orientations at all but the highest reductions are still closest to $(\bar{2}25)[5\bar{5}4]$ (ψ = 0, θ = 29.5, and φ = 45 deg).

IV. CONCLUSIONS

1. No significant differences could be found in the type or strength of textures developed when AA 3004 was rolled at 20 °C and 220 °C. When rolled at 400 °C and 520 °C, the effects of roll quenching and interpass recrystallization affected the strength of the deformation texture and modified the balance of texture components present.
2. Roll quenching caused a strengthening of the texture at the slab midplane during elevated temperature rolling due to the relatively lower flow stress associated

with the temperature gradient developed. At successively higher reductions (decreasing gage), however, the roll quenching had a negative effect on texture development due to the greater propensity for interpass reheat recrystallization.

3. In the early stages of deformation, AA 3004 appears to deform under mainly F (Taylor-type) conditions, as both the type and strength of orientations could be accounted for adequately well. Some Sachs-type deformation conditions also appeared to exist at low reductions, which explained the presence of a peak at the brass component.
4. At moderate to high reductions, the Taylor model with both full and relaxed constraints gave good predictions of the experimental data. The shift from the T component $\{4\ 4\ 11\}\langle 11\ 11\ 8\rangle$ toward the Cu component $\{112\}\langle 111\rangle$, observed at the highest reductions in the 20 deg rolled material, was predicted by the C model (ε_{NR} shears allowed).
5. The brass component was found to be a stable or metastable orientation in the string of rolling texture components, as it appeared in appreciable strengths at low reductions and increased with increasing reduction.
6. The cube texture formed in small quantities during interpass reheat recrystallization.

ACKNOWLEDGMENTS

The authors gratefully acknowledge the financial support provided by the ALCOA Technical Center, Pittsburgh, PA 15069. Thanks are also due to E. Llewellyn, J.C. Casato, W.G. Fricke, and S. Panchanadeeswaran for their help in preparing the data and to J. Hirsch and K. Lücke for supplying a manuscript of their paper prior to publication.

REFERENCES

1. I.L. Dillamore and W.T. Roberts: *Metall. Rev.*, 1965, vol. 10, p. 271.
2. G.E.G. Tucker: *Acta Metall.*, 1961, vol. 9, p. 275.
3. K. Lücke and J. Hirsch: *Proc. Aluminium Technology '86*, March 1986, T. Sheppard, ed., The Institute of Metals, London, p. 267.
4. J. Hirsch and K. Lücke: *Acta Metall.*, 1988, vol. 36 (11), pp. 2803-904.
5. R.J. Roe: *J. Appl. Phys.*, 1965, vol. 36, p. 2024.
6. K. Lücke, J. Pospiech, K.H. Virnich, and J. Jura: *Acta Metall.*, 1981, vol. 29, p. 167.
7. J. Hirsch, K. Lücke, and H. Mecking: *ICOTOM 7*, Sept. 1984, Noordwijerhout, The Netherlands, p. 7.
8. K. Lücke: *ICOTOM 6*, Sept.–Oct. 1981, Tokyo, Japan, The Iron and Steel Inst. of Japan, vol. 1, p. 14.
9. H.J. McQueen and H. Mecking: *Z. Metallkd.*, 1987, vol. 78 (5), p. 387.
10. J.S. Kallend: Ph.D. Thesis, University of Cambridge, England, 1970.
11. C.S. Da Costa Viana: Ph.D. Thesis, University of Cambridge, England, 1978.
12. M. Hatherly and K. Brown: *J. Austr. Inst. Metals*, 1966, vol. 11, p. 264.
13. G. Sachs: *Z. ver Dent. Eng.*, 1928, vol. 72, p. 734.
14. G.I. Taylor: *J. Inst. Metals*, 1938, vol. 62, p. 307.
15. A. Kochendorfer: *Reine and Angewandte Metallkunde*, Springer, Berlin, 1941, pp. 22-35.
16. G.E.G. Tucker: *Acta Metall.*, 1964, vol. 12, p. 1093.
17. A. Molinari, G.R. Canova, and S. Ahzi: *Acta Metall.*, 1987, vol. 35, p. 2983.